A moment-based approach for DVH-guided radiotherapy treatment plan optimization

2013 Phys. Med. Biol. 58 1869

(http://iopscience.iop.org/0031-9155/58/6/1869)

IOP Publishing Physics in Medicine and Biology

Phys. Med. Biol. **58** (2013) 1869–1887 doi:10.1088/0031-9155/58/6/1869

A moment-based approach for DVH-guided radiotherapy treatment plan optimization

M Zarepisheh[1], M Shakourifar[2], G Trigila[3], P S Ghomi[4], S Couzens[4], A Abebe[5], L Noreña[6], W Shang[7], Steve B Jiang[1] and Y Zinchenko[4]

[1] Center for Advanced Radiotherapy Technologies and Department of Radiation Medicine and Applied Sciences, University of California San Diego, La Jolla, CA 92037, USA
[2] Department of Computer Science, University of Toronto, Toronto, ON M5S 2E4, Canada
[3] Courant Institute of Mathematical Sciences, New York University, NY 10012, USA
[4] Department of Mathematics and Statistics, University of Calgary, Calgary, AB T2N 1N4, Canada
[5] Department of Mathematics and Statistics, University of North Carolina, Greensboro, NC 27412, USA
[6] Department of Mathematics, University of Central Florida, Orlando, FL 32816, USA
[7] Department of Mathematics, University of Michigan, Ann Arbor, MI 48104, USA

E-mail: yzinchen@ucalgary.ca

Received 24 October 2012, in final form 27 January 2013
Published 27 February 2013
Online at stacks.iop.org/PMB/58/1869

Abstract

The dose–volume histogram (DVH) is a clinically relevant criterion to evaluate the quality of a treatment plan. It is hence desirable to incorporate DVH constraints into treatment plan optimization for intensity modulated radiation therapy. Yet, the direct inclusion of the DVH constraints into a treatment plan optimization model typically leads to great computational difficulties due to the non-convex nature of these constraints. To overcome this critical limitation, we propose a new convex-moment-based optimization approach. Our main idea is to replace the non-convex DVH constraints by a set of convex moment constraints. In turn, the proposed approach is able to generate a Pareto-optimal plan whose DVHs are close to, or if possible even outperform, the desired DVHs. In particular, our experiment on a prostate cancer patient case demonstrates the effectiveness of this approach by employing two and three moment formulations to approximate the desired DVHs.

(Some figures may appear in colour only in the online journal)

1. Introduction

The dose–volume histogram (DVH), specifying the percentage of volume of a given organ that receives radiation dose greater than or equal to a given amount, is of great importance in evaluating plan quality in radiotherapy treatment planning. Despite the clinical importance of DVH constraints, an explicit implementation of such prescriptions is often associated with a non-convex optimization problem that raises computational difficulties (Deasy 1997, Bednarz *et al* 2002), and to the best of our knowledge, the existing methods to handle these constraints

are either heuristic or computationally demanding. The first model has been introduced by Langer and Leong (1987) where they group critical structure voxels into two classes. One class is supposed to satisfy the constraint, and the other one can violate it. Then, a problem is formulated and solved for each combination of classes, and eventually the best configuration is selected by performing some comparisons. In later investigation, they improved the efficiency of their approach by reformulating the problem as a mixed integer programming problem (Langer *et al* 1990). Although the mixed integer approach proves to be more efficient than the first one, it is still computationally expensive. Morrill *et al* (1991) divide each critical structure into high-dose and low-dose subregion based on the distance to the tumor. Then, the DVH constraints are converted into regional dose constraints. This method is heuristic and does not provide a credible procedure to break down the critical structure into low-dose and high-dose subregions before optimization. Bortfeld *et al* (1997) add a penalty term in the original objective function proportional to the violation of the DVH constraints. Spirou and Chui (1998) modify the gradient-based optimization algorithm in order to handle the DVH constraints. This is not a standard gradient method and its mathematical properties, such as convergence and local or global optimality of the solution, have not been verified. Cho *et al* (1998) propose two heuristic methods. One uses a volume sensitive penalty function, and the other one is projection-based method. Romeijn *et al* (2006) use the concept of conditional value-at-risk to impose bounds on the tail averages of the differential DVHs of structures. Zhang and Merritt (2008) employ a greedy approach in which they solve a sub-problem in each iteration. Their method is mathematically rigorous, but the weighting factor adjustment is based on a time-consuming trial-and-error approach. Censor *et al* (2008) suggest a linear feasibility problem and then relax the bounds in a heuristic fashion to come up with a reasonable solution. Michalski *et al* (2004) write the DVH constraints as a feasibility problem, and then try to find a feasible solution with a projection-based method, while the set of solutions satisfying the proposed constraints does not necessarily contain all the solutions associated with the DVH constraints. For other DVH constraints related approaches, the reader is referred to Wu and Mohan (2000), Starkschall *et al* (2001), Chen *et al* (2002) and Dai and Zhu (2003).

In this paper, we propose an approach based on the moments of the appropriately defined random variable to replicate a desired set of DVH curves. We assume that the desired DVHs, from now on referred to as the reference DVH curves, are already available. One practical setting where this assumption is readily justified corresponds to adaptive radiotherapy, where the desired DVHs come from the initial treatment plan of the patient (Li *et al* 2012, Yan *et al* 1999), and automatic (or knowledge-based) treatment planning, where the reference DVH curves are extracted from the delivered plans of previously treated patient with similar geometries and the same treatment protocol (Appenzoller *et al* 2012, Wu *et al* 2011).

The conceptual idea of using multiple moments to approximate a desired DVH has been introduced by Zinchenko *et al* (2008). Here, we introduce a computationally tractable moment-based approach equipped with the following desirable properties.

- For a given structure, the approach targets replicating the entire reference DVH rather than conforming to a few partial dose–volume constraints corresponding only to some selected points on the DVH.
- If the reference DVH is feasible but not Pareto-optimal, i.e. can be further improved without sacrificing other structures of interest, then the approach generates a Pareto-optimal plan consistent with the reference DVH,
- If the desired DVH is overly restricting, i.e. is inconsistent with dose deposition matrix, then the algorithm generates a Pareto-optimal plan whose associated DVH is ‘close’ to the reference DVH.

The proposed approach has two stages where each stage includes solving a computationally tractable convex optimization problem. The approach is applied to a prostate cancer case, and the results are presented. Although from purely theoretical viewpoint the approach is guaranteed to generate a solution satisfying a relaxed version of the DVH constraints, empirically we observe a high degree of conformity with the reference DVH constraints and provide a discussion on why such an outcome is expected.

2. Moment-based approach

We assume a set of reference DVHs, one per structure of interest, is given by the planner. Our goal is to generate a plan whose DVHs are close to the reference ones, or possibly even better.

The moment approach is based on the fact that a given DVH is uniquely determined by its corresponding infinite sequence of moments (Zinchenko *et al* 2008). With this in mind, we aim to restrict the search space of all possible treatment plans to the ones corresponding to the reference moments only. In this manner, we are able to generate a plan with DVHs resembling the reference ones, or alternatively certify that no such plan exists.

Let us denote the deposition matrix, beamlet intensities and dose values by D, x and d, respectively, where D_{ij} represents the amount of energy deposited in voxel i at the unit intensity of bixel j. The following linear system in d, x describes all beamlet intensities and dose values consistent with the fixed dose deposition matrix:

$$\begin{cases} d = Dx, \\ x \geqslant 0. \end{cases}$$

We call any x, d satisfying the above *feasible*.

For a given structure, we call its reference DVH *feasible* if there exists a feasible x so that the resulting dose d produces an equivalent or better DVH. For example, for a given critical structure, the DVH corresponding to d coincides or lies below the reference DVH if plotted. Similarly, we call a set of DVHs *feasible* if all the DVHs may be simultaneously realized or improved by selecting an appropriate feasible x.

For the sake of notational simplicity, we assume that we have a single tumor—with voxel indices in $\mathcal{T}$—and a single critical structure—with voxel indices in $\mathcal{C}$. In order to distinguish between the doses associated with the tumor and critical structure with ease, we re-order the entries of D and d so that these may be partitioned as follows:

$$D = \begin{pmatrix} D_{\mathcal{T}} \\ D_{\mathcal{C}} \end{pmatrix}, \quad \mathrm{d} = \begin{pmatrix} \mathrm{d}_{\mathcal{T}} \\ \mathrm{d}_{\mathcal{C}} \end{pmatrix}.$$

For fixed k define

$$M^k(\mathrm{d}_{\mathcal{T}}) = \frac{1}{|\mathcal{T}|} \sum_{i \in \mathcal{T}} \mathrm{d}_i^k,$$

$$M^k(\mathrm{d}_{\mathcal{C}}) = \frac{1}{|\mathcal{C}|} \sum_{i \in \mathcal{C}} \mathrm{d}_i^k,$$

the kth-order *moments* of the dose d for the target and critical structure, where $|\mathcal{T}|$ and $|\mathcal{C}|$ are the numbers of voxels for the tumor and critical structure, respectively. Observe that the kth root of the moment function corresponds to a well-known kth generalized equivalent uniform dose (gEUD).

Let $\overline{d} \geqslant \mathbf{0}$ be some hypothetical and not necessarily feasible dose corresponding to the reference DVHs. We define the corresponding kth *reference moments* as

$$\overline{M}_{\mathcal{T}}^k = M^k(\overline{\mathrm{d}}_{\mathcal{T}}),$$

$$\overline{M}_{\mathcal{C}}^k = M^k(\overline{\mathrm{d}}_{\mathcal{C}}).$$

Remark. Note that the reference moments are defined based on a complete description of the underlying reference DVH. Specifically, the reference moments may be computed as the Riemann–Stieltjes-type integral of the corresponding monomials with respect to the DVHs, so strictly speaking the explicit knowledge of $\overline{d}$ is not required. For example, the k-reference moments for the critical structure can be computed as

$$\overline{M}_{\mathcal{C}}^{k} = -\int_{0}^{\mathrm{d}_{\max}} \delta^{k}\, \mathrm{dDVH}(\delta),$$

where $\mathrm{d}_{\max}$ represents the highest dose allowed to the structure and DVH is the reference DVH interpreted as a function of the dose returning the corresponding volume percentage. Alternatively, if $\overline{d}$ is still desired, a reference dose distribution may be reconstructed from the DVH function via its inverse transform. For instance, for a fixed structure, we may set the corresponding dose vector as $\bar{d}_i = \mathrm{DVH}^{-1}(1 - \frac{\mathrm{i}}{N})$ for $i = 1, \ldots, N$, where N is the number of voxels in the structure. Resulting $\overline{d}$ is not unique—any permutation of $\overline{d}$ would correspond to an identical DVH; yet note that the reference moments do not depend on which particular $\overline{d}$ is chosen, as the moments are symmetric functions of the dose. When the reference DVH is not readily available, it may be interpolated from a set of physician-prescribed partial dose–volume constraints corresponding to the so-called critical points on the DVH curve. For example, one may simply connect the critical points with linear segments, provided such an interpolation makes clinical sense. In the case when this interpolation is too coarse, one may introduce a few more additional critical points to the DVH description and repeat the procedure until a reasonable reference DVH is recovered.

Based on the earlier mentioned moments-to-distribution equivalence, our goal of finding the beamlet intensities x that result in dose d matching the reference DVHs may be mathematically re-formulated as a nonlinear feasibility problem:

$$\begin{cases} d = Dx, & x \geqslant 0 \\ M^{k}(\mathrm{d}_{\mathcal{C}}) = \overline{M}_{\mathcal{C}}^{k}, & k = 1, \ldots, \infty, \\ M^{k}(\mathrm{d}_{\mathcal{T}}) = \overline{M}_{\mathcal{T}}^{k}, & k = 1, \ldots, \infty. \end{cases} \tag{1}$$

However, solving the feasibility problem above presents two major challenges.

Firstly, the number of constraints is infinite. To overcome this in practice, we limit the range of k only to finitely many values. This reduction step is closely related to a well-known 'moment problem' in applied mathematics and relies on the fact that a probability distribution can often be described fairly accurately using only a finite moment subsequence; see the appendix for more details.

Secondly, the specified constraints are non-convex, despite the fact that the moments themselves are convex functions in their domain $d \geqslant 0$. The problem is the equalities in the constraint specification.

In the case of the critical structure, to resolve the latter problem, we note that lower doses are preferred. Therefore, given the fact that moments are convex and increasing in dose, we replace

$$M^{k}(\mathrm{d}_{\mathcal{C}}) = \overline{M}_{\mathcal{C}}^{k}$$

by

$$M^{k}(\mathrm{d}_{\mathcal{C}}) \leqslant \overline{M}_{\mathcal{C}}^{k}$$

to achieve not only the convexity of the constraint, but also an equal or a better degree of consistency with the corresponding gEUD-type requirement.

Since we are generally interested in producing high nearly homogeneous dose for the target, the above consideration cannot be directly applied to the tumor constraints. However,

the following modifications work. Note that for $k = 1$, the constraint is linear (and so is convex) and thus we leave

$$M^1(\mathrm{d}_{\mathcal{T}}) = \overline{M}^1_{\mathcal{T}}$$

as is. For $k > 1$, we use the prescription dose to the tumor p and replace the kth moment function $M^k(\mathrm{d}_{\mathcal{T}})$ with its shifted variant $M^k(\mathrm{d}_{\mathcal{T}} - p\mathbf{1})$ where $\mathbf{1}$ is the vector of 1s. The reference moments for the tumor are also modified accordingly, and we still denote these shifted reference moment values with the same symbol $\overline{M}^k_{\mathcal{T}}$, $k > 1$, slightly abusing the notation. Now, since our objective is to get closer to the prescription dose value p, we conclude that smaller values of $M^k(\mathrm{d}_{\mathcal{T}} - p\mathbf{1})$ are desirable for even k. Not only that, for positive even values of k the function $M^k(\mathrm{d}_{\mathcal{T}} - p\mathbf{1})$ is convex. So for $k > 1$ and for even values of k, we replace the original tumor constraints with

$$M^k(d_{\mathcal{T}} - p\mathbf{1}) \leqslant \overline{M}^k_{\mathcal{T}}$$

and ignore all odd $k > 1$.

Remark. It is worth mentioning that if we require all the even-order dose moments being equal to the reference values only, we are still guaranteed to recover the reference DVH precisely. The reason for this is that the even-order moments describe the distribution of the square of the dose, and since the dose is positive, it is equivalent to describing the dose itself. In turn, if applied to the tumor with shifted even moments, the equality constraints would guarantee the recovery of the tumor DVH equivalent to the reference DVH in terms of its deviations from the prescription dose p.

Putting the constraints together, we can formulate a convex relaxation for problem (1) as follows:

$$\begin{cases} M^k(D_{\mathcal{C}}x) \leqslant \overline{M}^k_{\mathcal{C}}, & k = 1, 2, \ldots, K_{\mathcal{C}}, \\ M^j(D_{\mathcal{T}}x - p\mathbf{1}) \leqslant \overline{M}^j_{\mathcal{T}}, & j = 2, 4, 6, \ldots, 2K_{\mathcal{T}}, \\ M_1(D_{\mathcal{T}}x) = \overline{M}^1_{\mathcal{T}}, \\ x \geqslant 0, \end{cases} \tag{2}$$

where $K_{\mathcal{C}}$ and $K_{\mathcal{T}}$ are fixed positive integers.

Despite its theoretical and practical importance, the feasibility problem (2) still has two limitations from the end-user viewpoint. Firstly, if the above problem is infeasible, that is, when the corresponding moment (or gEUD-type) constraints are simply too restrictive when imposed simultaneously, after attempting to solve the problem the user is left with no other useful information besides the fact that it cannot be done. Secondly, if the problem is feasible and has alternative solutions, the model is not encouraged to find the Pareto one.

Our aim is to present an approach that is capable of handling both feasible and infeasible sets of reference DVHs as specified below.

Phase I. Attempt to find beamlet intensities x that produce dose d consistent with the reference DVH in terms of its moments. In the case when the reference moment constraints are infeasible, provide the nearest plan consistent with the reference DVH.

Phase II. If the reference moment constraints are feasible, then provide the Pareto beamlet weights x and the dose distribution d amongst all the feasible solutions.

The main idea behind implementing Phases I and II is to change, in an adaptive way, the bounds on the moments in (2).

2.1. Phase I

Suppose that the reference set of DVHs is infeasible. In this case, problem (1) does not admit any feasible solution, and its relaxed version (2) may or may not admit a feasible solution. In the latter case, the question that arises is that of how to provide a treatment plan that is somehow close to the reference DVH.

Consider the following optimization problem:

$$\begin{cases} \min_{x,\alpha,\beta} \sum_j \alpha_j + \sum_k \beta_k \\ M^k(D_{\mathcal{C}}x) \leqslant \overline{M}^k_{\mathcal{C}} + \beta_k, & k = 1, 2, \ldots, K_{\mathcal{C}}, \\ M^j(D_{\mathcal{T}}x - p\mathbf{1}) \leqslant \overline{M}^j_{\mathcal{T}} + \alpha_j, & j = 2, 4, 6, \ldots, 2K_{\mathcal{T}}, \\ M^1(D_{\mathcal{T}}x) = \overline{M}^1_{\mathcal{T}}, \\ x,\ \beta_k,\ \alpha_j \geqslant 0. \end{cases} \tag{3}$$

In this formulation, we loosen the bounds on the moments by introducing the surplus variables α_j and β_k (compare with (2)). At the same time, we enforce these variables to be as small as possible by integrating them in the objective function.

2.2. Phase II

Suppose that problem (2) admits one or more feasible solutions. In this case the natural question to address is: How we select, among the set of feasible solutions, the solution which is characterized by the smallest dose of radiation to the organs and the closest dose to the tumor?

The main idea is to shrink the moment bounds in problem (2) as much as possible while keeping the feasibility. This motivates our next formulation:

$$\begin{cases} \max_{x,\alpha,\beta} \sum_j \alpha_j + \sum_k \beta_k \\ M^k(D_{\mathcal{C}}x) \leqslant \overline{M}^k_{\mathcal{C}} - \beta_k, & k = 1, 2, \ldots, K_{\mathcal{C}}, \\ M^j(D_{\mathcal{T}}x - p\mathbf{1}) \leqslant \overline{M}^j_{\mathcal{T}} - \alpha_j, & j = 2, 4, 6, \ldots, 2K_{\mathcal{T}}, \\ M^1(D_{\mathcal{T}}x) = \overline{M}^1_{\mathcal{T}}, \\ x,\ \beta_k,\ \alpha_j \geqslant 0. \end{cases} \tag{4}$$

Non-negative variables α and β are introduced in order to tighten the bounds on the moments' inequalities. Maximizing the objective function enforces the bounds to become as tight as possible. The Pareto optimality in terms of the dose distribution (Zarepisheh *et al* 2012) is guaranteed in the above problem since the radiation doses in critical structures' voxels are encouraged to decrease as much as possible and the radiation doses in tumor's voxels are encouraged to get close to the prescription dose as much as possible. In other words, in the optimal solution, it is impossible to improve the radiation doses in some voxels without worsening those in other voxels (improvement of doses in tumor's voxels means getting closer to the prescribed dose, while that in voxels in critical structures means delivering less radiation).

2.3. Two-phase algorithm

We are ready to describe how, combining Phases I and II, we can devise a strategy for finding an optimal plan. The strategy is illustrated by the flowchart in figure 1.

Given a set of DVHs that can be either feasible or infeasible, we first execute Phase I as described in section 2.1. If the objective function $\sum_j \alpha_j + \sum_k \beta_k$ reaches zero, we have found a solution that is feasible for problem (2) and problem (4). Thus, we may execute Phase II of the algorithm in order to possibly improve the plan quality by tightening the moment bounds.

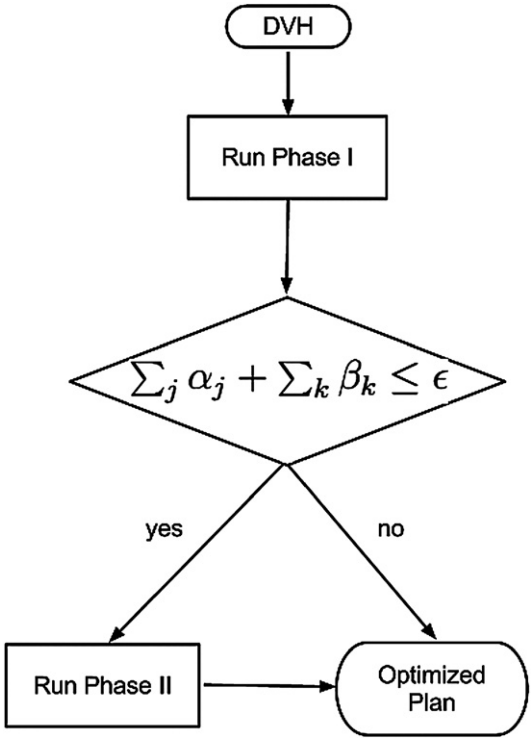

Figure 1. Flowchart of the algorithm. Phase I attempts to find the beamlet intensities that produce dose consistent with the reference DVH in terms of its moments. If the optimal objective function is less than ϵ, then Phase II tries to find the Pareto-optimal solution amongst all the feasible solutions.

It should be noted that in practical implementation, since we have to use an iterative algorithm with some finite termination criteria and finite-precision numerics, the optimal value of the objective function in Phase I may not reach zero even in the feasible case. Hence, we replace zero with a small threshold ϵ to discriminate between the feasible and infeasible cases.

3. Numerical results and discussion

In this section, we illustrate the performance and reliability of our proposed approach on a prostate cancer patient. The number of voxels and bixels are 50 221 and 943, respectively. We use different number of moments and consider both feasible and infeasible sets of reference DVH curves to justify the strategies and heuristics we have adopted in our implementation.

We implemented our algorithm in Matlab using the constrained minimization routine `fmincon`. We provided the gradient information to the `fmincon`, for both the constraints and objective function, which resulted in a significant improvement in the performance of the algorithm. The interior point method has been selected to solve the problem. We ran the code on a PC with Intel Core i7 3.40 GHz CPU and 12 GB RAM.

3.1. Feasible set of reference DVHs

Figures 2 and 3 depict the results of our algorithm when using two ($K_{\mathcal{C}} = K_{\mathcal{T}} = 2$) and three ($K_{\mathcal{C}} = K_{\mathcal{T}} = 3$) moments, respectively, with feasible reference set of DVHs.

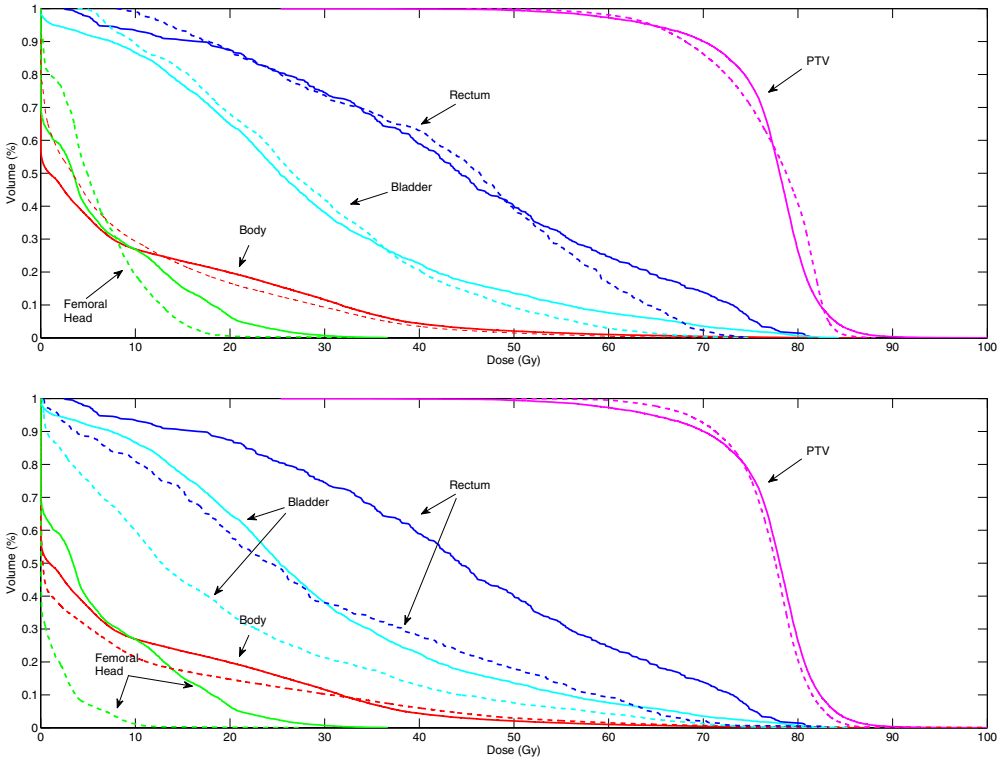

Figure 2. Results relative to Phase I (upper) and Phase II (lower) when using two moments. The solid and dashed lines represent the reference and computed DVH curves, respectively.

As can be seen in the figures, the results obtained using Phase II is characterized by a smaller dose delivered to healthy organs and closer dose to a prescription value for PTV compared to what is obtained using Phase I of the algorithm. The running time in our system was 64 s (Phase I) and 215 s (Phase II) for two moments, and 42 s (Phase I) and 205 s (Phase II) for three moments.

The results obtained from three moments are slightly better than those from two moments, although this may not be quite evident by visually analyzing the figures. To support the last claim, we quantify the area where the computed DVHs from two and three moments are worse than the reference DVHs. The results from Phase II in figures 2 and 3 indicate that the computed DVHs are worse than the reference ones for two structures only, namely there is a slightly higher volume exposed to the higher doses for body, and a slight underdose to PTV as compared to the prescription dose. Evaluated numerically, the corresponding areas of these parts are 1.9534 (1.6155) and 0.4349 (0.3610) for the dose computed with two (three) moments. Therefore, employing three moments leads to slightly better approximation in this case.

3.2. Infeasible set of reference DVHs

To get an infeasible set of DVHs, we manually improve some parts of the Pareto-optimal plan generated by the quadratic model. Since the plan generated by the quadratic model is Pareto-optimal in terms of the DVH (Zarepisheh *et al* 2012), it becomes infeasible if we improve any part of it with no other changes to the DVHs.

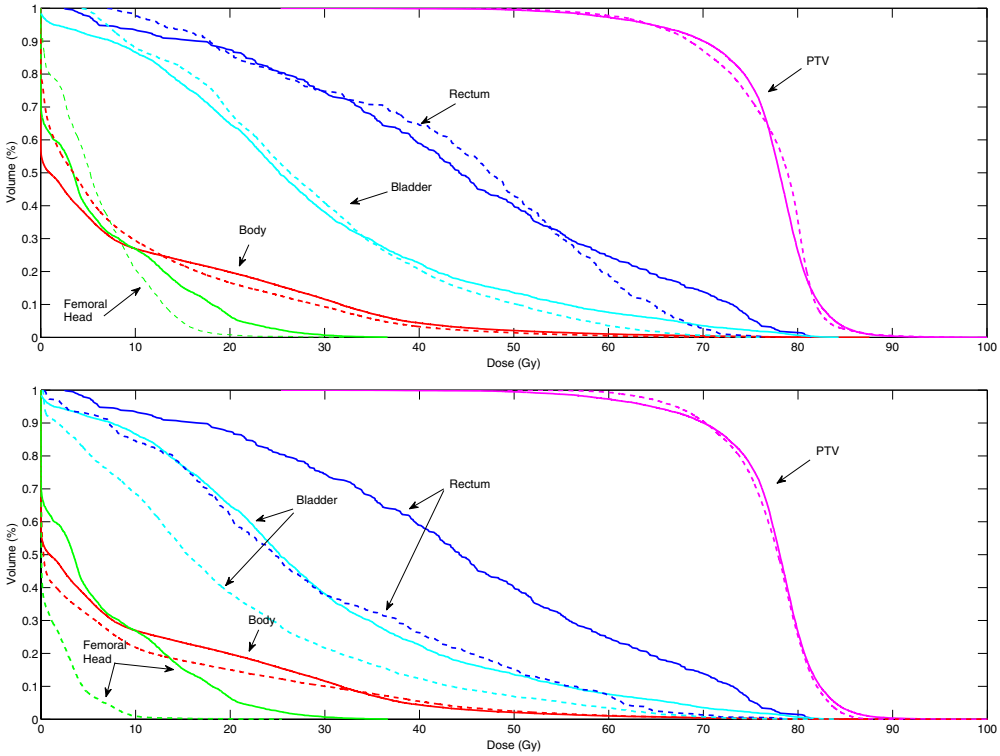

Figure 3. Results relative to Phase I (upper) and Phase II (lower) when using three moments. The solid and dashed lines represent the reference and computed DVH curves, respectively.

We tested the robustness of our approach on three different infeasible sets of reference DVHs (figures 4), 5 and 6, respectively). The infeasible sets of reference DVHs for the three cases considered were generated as follows.

(i) Starting from the Pareto-optimal DVH obtained by the quadratic model, we obtained the DVHs (solid lines) in figure 4 by shifting the DVH curve associated with the PTV overdose and underdose toward the prescription dose of 79.3 Gy.

(ii) Starting from the DVH curves described in point (i), we obtained a new set of DVHs (solid lines in figure 5) by shifting the DVH curve associated with the body to the left (in red).

(iii) Starting from the DVH curves described in point (ii), we obtained a new set of DVHs (solid lines in figure 6) by further shifting the DVH curve corresponding to the rectum to the left.

As we can see from figures 4–6 the approach performs well with infeasible sets of DVHs. In particular, the numerical solution that was obtained after Phase I is not far from the reference DVHs, reflecting the fact that among all the feasible solutions Phase I finds the solution that is closest to the reference DVHs in terms of deviation from the bounds characterized by problem (3). The running times in the infeasible scenarios were 287 s, 288 s and 287 s for the first, second and the third scenarios, respectively.

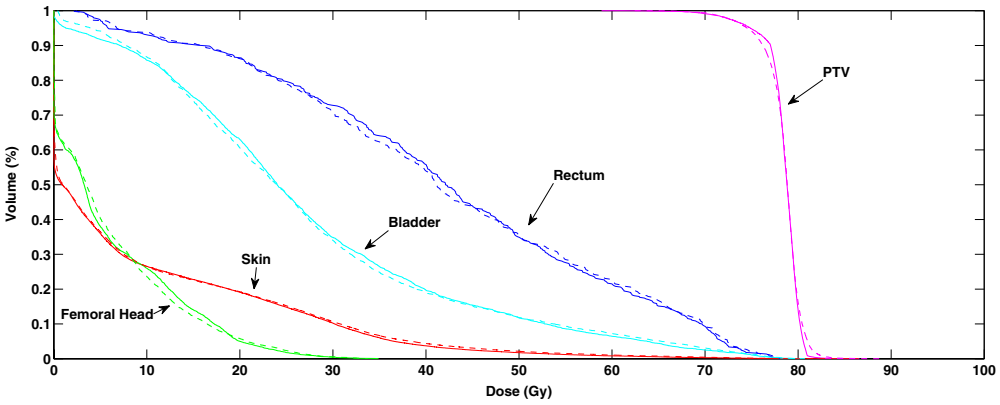

Figure 4. The infeasible reference DVH curves obtained by shifting the PTV's DVH toward the prescription dose. The solid and dashed lines represent the reference and computed DVH curves, respectively.

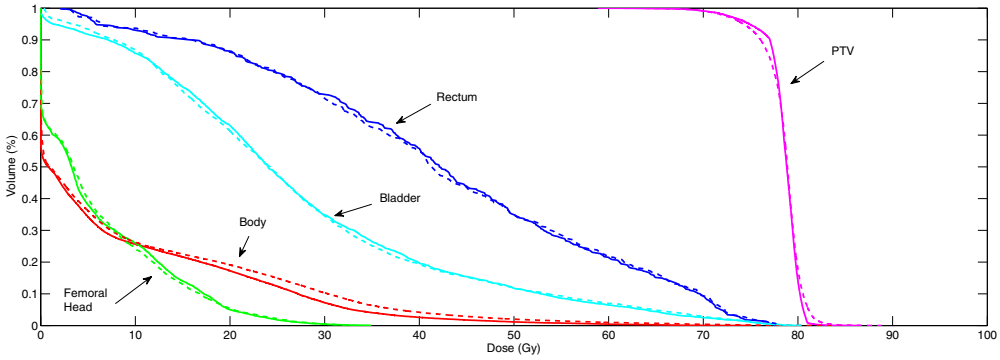

Figure 5. The infeasible reference DVH curves obtained by shifting the PTV's DVH toward the prescription dose, the body's DVH toward left. The solid and dashed lines represent the reference and computed DVH curves, respectively.

3.3. Discussion

Since our approach is designed to work with both feasible and infeasible set of reference DVHs in Phase I, naturally one may ask whether taking the idealized dose distribution—zero dose to all organs at risk and a uniform prescription dose to the target—as the reference set of DVHs would generate any serviceable results.

We ran a set of numerical experiments where Phase I was initiated with the idealized reference dose distributions, yet the resulting dose distributions were not good. The explanation behind this is that the 'distance' between the idealized dose and the set of all feasible doses is too great to produce a meaningful computational result with relatively little effort on users part. When the reference set of DVHs is infeasible, our approach finds a projection of that point onto the Pareto surface of all achievable dose distributions. If the reference set of DVHs is too far from the feasible region, then the resulting projection may not be practically meaningful, since, for example, there is no way to instruct our model and the optimization algorithm as to

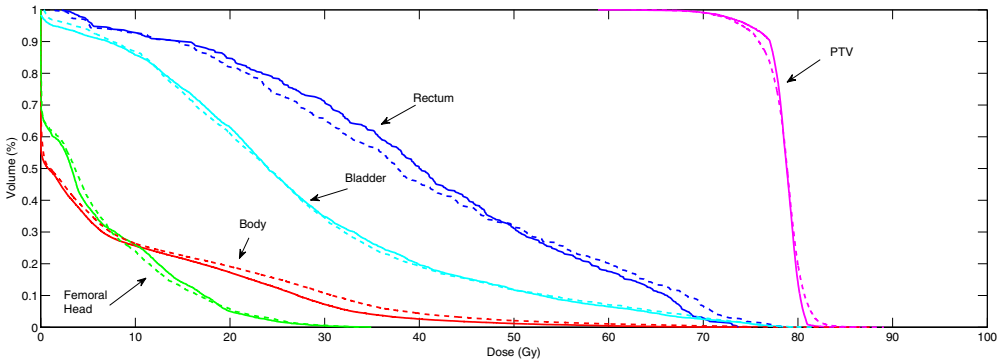

Figure 6. The infeasible reference DVH curves obtained by shifting the PTV's DVH toward the prescription dose, the body's and rectum's DVH toward left. The solid and dashed lines represent the reference and computed DVH curves, respectively.

which parts of the idealized dose distribution are more valuable than the others. As a result, the computed solution may not be serviceable.

Next we provide some insights into why our approach performed as well as it did, in spite of the fact that formulation (2) subsequently giving rise to the two phases presented, is a relaxation of the exact DVH formulation (1), and comment on some possible extensions.

Recall that from a theoretical viewpoint the dose distribution arising from solving (1), if this problem is feasible, is guaranteed to exactly coincide with the reference DVHs. In fact, even if we consider only K finitely many first moments instead, as K grows larger the resulting distributions become visually indistinguishable from the set of reference DVHs.

On the other hand, a solution to (2) does not necessarily reproduce the desired set of DVHs since the equality moment conditions are relaxed into inequalities. However, despite possibly missing the reference DVHs, such a solution is always guaranteed to satisfy a set of reference moment constraints, which in turn are equivalent to a set of corresponding gEUD requirements—one favorable feature of the presented approach.

Remark. Note that even solving the so-called partial dose–volume constraint mixed integer programming formulation, which is notoriously computationally difficult to work, does not warrant that the planner will obtain a DVH he or she is targeting in the first place. The reason why such a guarantee is lacking is that the partial dose–volume constraints limit the volume exposure only at one particular dose level, and say nothing about what may happen for the nearby doses, no matter how close they are to each other. In this respect, attempting to reproduce the whole DVH may be more clinically relevant as compared to targeting just a few points on the DVH. It is worthwhile mentioning that despite the inequality-type constraints, Phase I encourages equalities with respect to the reference moments, and recall that a linear objective function posed over a closed convex set achieves its extremum at the boundary of the feasible region. For our formulations (3) this implies that at least some of the nonlinear constraints will be met with equalities. Consequently, the equality to reference moments will induce the proximity of the resulting dose distribution to the reference set of DVHs—the behavior we observed in our numerical experiments.

For our prostate case, we note that using only two or three moments suffices to obtain a good approximation of the reference DVH. However, the question 'how many moments do we need to use?' still remains unanswered, and is a topic of future experimental and theoretical investigation.

A few comments on the numerical stability and possible extensions of the approach are due as well. In our implementation, we found that using

$$\frac{M^k(D_{\mathcal{C}}x)}{\overline{M}^k_{\mathcal{C}}} \leqslant 1 \pm \beta_k$$

instead of

$$M^k(D_{\mathcal{C}}x) \leqslant \overline{M}^k_{\mathcal{C}} \pm \beta_k,$$

and likewise for the target, results in far greater numerical stability of the Matlab solver. This is not surprising as the alternative re-scaling takes care of numerical ill-conditioning of the constraint by avoiding extremely large values of the left- and right-hand sides especially for large k.

In attempt to reduce the total optimization runtime, one may explore merging the models in Phases I and II into a single 'big-M'-type formulation,

$$\begin{cases} \min_{x,\underline{\alpha},\underline{\beta},\overline{\alpha},\overline{\beta}} \; M\left(\sum_j \overline{\alpha}_j + \sum_k \overline{\beta}_k\right) - \left(\sum_j \underline{\alpha}_j + \sum_k \underline{\beta}_k\right) & \\ M^k(D_{\mathcal{C}}x) \leqslant \overline{M}^k_{\mathcal{C}} + \overline{\beta}_k - \underline{\beta}_k, & k = 1, \ldots, K_{\mathcal{C}}, \\ M^j(D_{\mathcal{T}}x - p\mathbf{1}) \leqslant \overline{M}^j_{\mathcal{T}} + \overline{\alpha}_j - \underline{\alpha}_j, & j = 2, \ldots, 2K_{\mathcal{T}}, \\ M^1(D_{\mathcal{T}}x) = \overline{M}^1_{\mathcal{T}}, & \\ x,\ \underline{\beta}_k,\ \underline{\alpha}_j,\ \overline{\beta}_k,\ \overline{\alpha}_j \geqslant 0, & \end{cases} \tag{5}$$

where M is some fixed large number—an optimization technique that already recommended itself quite well in the early days of linear optimization, and recently in nonlinear optimization (Zarepisheh and Khorram 2011). Note that for sufficiently large M the model will first enforce reference moments feasibility by focusing on minimizing the big-M term in the objective, $\sum_j \overline{\alpha}_j + \sum_k \overline{\beta}_k$. In turn, only if it is possible to set the big-M term close to zero, the model will further move onto pushing the moments beyond their reference values in search of an even better plan by maximizing the leftover objective term, $\sum_j \underline{\alpha}_j + \sum_k \underline{\beta}_k$.

Ultimately, we expect that our approach may be suited to finding a better starting point—a feasible plan better conforming to the reference set of DVHs—when planning for an optimal radiotherapy. However, determining a good starting point may not fully eliminate the need for some further user-assisted tweaking of the plan's parameters. In this regard, in addition to adaptively changing the reference DVHs, we suggest using a weighted moment-based objective function for either of the described phases. Namely, depending on the phase, one may desire to minimize or maximize

$$\sum_j v_j \alpha_j + \sum_k w_k \beta_k,$$

where the user is allowed to execute multiple optimization runs while manually changing the moment weights v, w based on the perceived relative clinical importance of the moment constraints.

4. Conclusion

In this paper, we present a new approach for replicating the set of reference DVHs in radiotherapy treatment optimization. Our ideas may be used not only in IMRT, but in any other radio-therapeutic platform such as volumetric-modulated arc therapy, etc. The proposed algorithm is based on the idea of approximating the reference dose distribution with finitely few moment constraints imposed on the dose.

As opposed to a precise mixed integer programming implementation of the partial-volume constraints, our moment-based approach is based on convex optimization techniques and therefore may lead to much faster recovery of and improvement over the reference DVH. In turn, the reference DVH curves may come, for example, from the initial treatment plan of the patient in the case of adaptive therapy, or may be constructed from plans of previous treated patients with similar geometries and same treatment protocol.

Acknowledgments

The authors would like to express their thanks to IMA (Institute for Mathematics and its Applications) and PIMS (Pacific Institute for the Mathematical Sciences) for holding a 10-day workshop on Mathematical Modeling in Industry in Calgary, Canada. This study was largely accomplished during this workshop where MZ was the industrial mentor and YZ was the mathematical advisor. We are also very grateful for the valuable comments and suggestions made by the anonymous reviewers.

Appendix. Elementary moment-based DVH bounds

The aim of the appendix is to demonstrate how the partial knowledge of the reference moments affects the resulting DVH. For the sake of simplicity, we do not focus on deriving the most accurate bounds on the DVH imposed by the reference moments, but rather rely on some well-known facts from the probability theory. We hope that the material that follows will serve as an illustration to how the quality of our moment-based approximation of the reference DVH can be analyzed rigorously.

Recall that for a given structure, its DVH is equivalent to a cumulative probability distribution of some properly defined random variable representing the dose (Zinchenko *et al* 2008). Specifically, simplifying our notation even further and assuming we have only one structure of interest with dose vector d, the setup is as follows. For $d \in \Re^n$ fixed, we define a random variable $\widetilde{D}$ with values d_i, $i = 1, n$, each occurring with equal probability $1/n$. The cumulative distribution function F of $\widetilde{D}$ at a point t is defined as probability that $\widetilde{D} \leqslant t$, $F(t) = \Pr(\widetilde{D} \leqslant t)$. Now, the DVH value at the dose level t may be defined as $\mathrm{DVH}(t) = 1 - F(t)$.

With the above in mind, the problem of restricting d so that we obtain a given reference DVH may be equivalently viewed as a problem of producing a random variable $\widetilde{D}$ with predetermined probability distribution. In order to accomplish the latter, one may rely on moments of $\widetilde{D}$.

Taking this probabilistic outlook on our problem, we first introduce some preliminaries necessary to derive closed-form bounds on the DVH given its first two and three moments. Next we demonstrate how these bounds apply to one particular set of the reference DVHs, and finally we remark on a few metrics that may be used to judge the quality of the moment-based approximation to the DVH.

Chebyshev and Markov inequalities, closed-form bounds

Let the first three moments of $\widetilde{D}$ be denoted as

$$\overline{M}^1 = \frac{1}{n}\sum_{i=1}^{n} d_i,$$

$$\overline{M}^2 = \frac{1}{n}\sum_{i=1}^{n} d_i^2,$$

$$\overline{M}^3 = \frac{1}{n}\sum_{i=1}^{n} d_i^3.$$

The variance of $\widetilde{D}$ is defined as the square of the standard deviation σ,

$$\sigma^2 = \overline{M}^2 - (\overline{M}^1)^2.$$

Our DVH bounds with two moments $\overline{M}^1, \overline{M}^2$ rely on the so-called one-sided Chebyshev inequalities valid for any random variable X,

$$\Pr(X \geqslant \overline{M}^1 + a) = \Pr(X \leqslant \overline{M}^1 - a) \leqslant \frac{\sigma^2}{a^2 + \sigma^2},$$

which in turn may be derived from the well-known Markov inequality,

$$\Pr(|X| \geqslant a) \leqslant \frac{\mathrm{E}(|X|)}{a},$$

with $\mathrm{E}(|X|)$ denoting the first moment of $|X|$ also known as the expectation.

Remark. Markov inequality follows directly from the definition of expectation.

Since the derivation of Chebyshev inequalities is fairly compact, for the sake of self-containment we present it below. Note that for τ such that $a + \tau > 0$ we may write

$$\begin{aligned}
\Pr(X - \overline{M}^1 \geqslant a) &= \Pr(X - \overline{M}^1 + \tau \geqslant a + \tau) \\
&= \Pr\left(\frac{X - \overline{M}^1 + \tau}{a + \tau} \geqslant 1\right) \leqslant \Pr\left(\left(\frac{X - \overline{M}^1 + \tau}{a + \tau}\right)^2 \geqslant 1\right) \\
&\leqslant \mathrm{E}\left(\left(\frac{X - \overline{M}^1 + \tau}{a + \tau}\right)^2\right) \\
&= \frac{\sigma^2 + \tau^2}{(a + \tau)^2},
\end{aligned}$$

where the next to last transition follows from Markov inequality. Now, in order to obtain the tightest bound we can minimize the final term above with respect to τ subject to $a + \tau > 0$, for example, by setting to zero its first derivative. This gives us the critical value

$$\tau^* = \frac{\sigma^2}{a}.$$

Substituting τ^* and simplifying, we obtain one-sided Chebyshev inequality

$$\Pr(X \geqslant \overline{M}^1 + a) \leqslant \frac{\sigma^2}{a^2 + \sigma^2},$$

with the other bound derived in a similar fashion.

Now, applying DVH-to-probability distribution equivalence, we can use one-sided Chebyshev inequalities to obtain the following bounds on the DVH when the first two reference moments $\overline{M}^1, \overline{M}^2$ are prescribed:

$$\underline{\mathrm{DVH}}(t) = \begin{cases} 1 - \frac{\sigma^2}{(\overline{M}^1 - t)^2 + \sigma^2}, & \text{if } t \leqslant \overline{M}^1, \\ 0, & \text{if } t > \overline{M}^1, \end{cases}$$

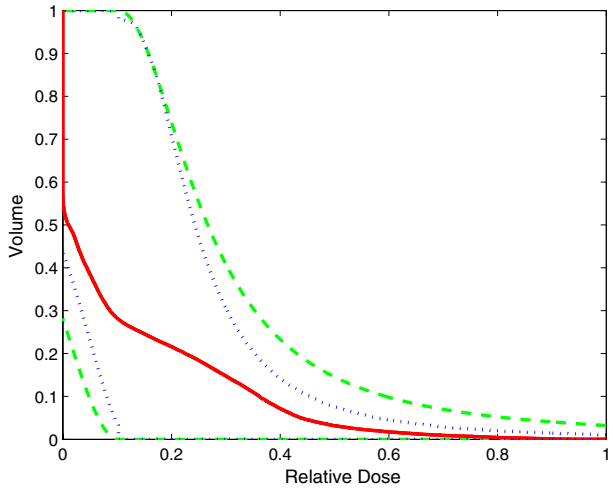

Figure A1. Error bounds for a critical structure; two outer-dashed curves correspond to two moments, two inner doted curves to three moments, and mid solid curve to the reference DVH; dose is varied from 0 to 83 Gy.

$$\overline{\mathrm{DVH}}(t) = \begin{cases} 1, & \text{if } t \leqslant \overline{M}^1, \\ \frac{\sigma^2}{(\overline{M}^1 - t)^2 + \sigma^2}, & \text{if } t > \overline{M}^1. \end{cases}$$

That is, given that the first two moments corresponding to d are required to be equal to the reference moment values $\overline{M}^1, \overline{M}^2$, the DVH resulting from d is guaranteed to satisfy

$$\underline{\mathrm{DVH}}(t) \leqslant \mathrm{DVH}(t) \leqslant \overline{\mathrm{DVH}}(t), \ \forall t,$$

see figures A1 and A2. Observe that since the variance associated with the target volume is much smaller than the variance associated with the critical structure, the corresponding bounds on the target DVH are also much tighter. Also, the target DVH bounds do not improve significantly with the addition of third-order reference moment constraint.

Note that the lower and upper bounds $\underline{\mathrm{DVH}}(t)$ and $\overline{\mathrm{DVH}}(t)$ remain valid even if we relax the second reference moment constraint into an inequality. That is, with the average dose to a structure being fixed, further reduction of the second moment—equivalently the standard deviation σ—produces tighter bounds $\underline{\mathrm{DVH}}(t)$, $\overline{\mathrm{DVH}}(t)$, which can be easily verified with the corresponding formulas.

In a similar fashion, when three reference moments are prescribed, we may use, for example, concentration-type inequalities derived in Bertsimas and Popescu (2005), and obtain even tighter bounds on the DVH we aim to reproduce. Namely, defining

$$\alpha = \frac{\overline{M}^2 - (\overline{M}^1)^2}{(\overline{M}^1)^2},$$

$$\beta = \frac{\overline{M}^1 \overline{M}^3 - (\overline{M}^2)^2}{(\overline{M}^1)^4},$$

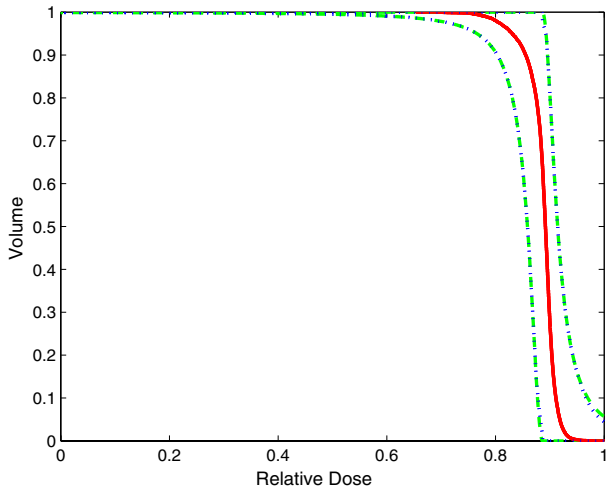

Figure A2. Error bounds for a target volume; two outer dashed curves correspond to two moments, two inner doted curves to three moments, and mid solid curve to the reference DVH; dose is varied from 0 to 87 Gy.

for $t \geqslant 0$ we may write[8]

$$\underline{\mathrm{DVH}}(t) = \begin{cases} \max\left(\frac{(\alpha-\gamma_t)^3}{(\beta+(1+\alpha)(\alpha-\gamma_t))(\beta+(\alpha-\gamma_t)^2)},\ 1-\frac{\alpha}{\alpha+\gamma_t^2}\right), & \text{if } t \leqslant \overline{M}^1, \\ 0, & \text{if } t > \overline{M}^1, \end{cases}$$

and

$$\overline{\mathrm{DVH}}(t) = \begin{cases} 1, & \text{if } t \leqslant \overline{M}^1, \gamma_t \leqslant \alpha, \\ \min\left(\frac{\alpha}{\alpha+\gamma_t^2},\ \frac{1}{1+\gamma_t}\ \frac{\beta}{\alpha+\beta-\gamma_t^2)}\right), & \text{if } t \leqslant \overline{M}^1, \gamma_t > \alpha, \\ \frac{1}{1+\gamma_t}\ \frac{\beta+(1+\gamma_t)(\alpha-\gamma_t)}{\beta+(1+\alpha)(\alpha-\gamma_t)}, & \text{if } t > \overline{M}^1, \end{cases}$$

where

$$\gamma_t = 1 - \frac{t}{\overline{M}^1},$$

see figures A1 and A2.

In our derivations, we did not account for the fact that the dose is non-negative, may take values only on some finite interval, that is, has a technologically or clinically limited maximal value, and moreover is determined from the dose deposition matrix. Thus, the presented bounds are still loose in a sense that the actual restrictions imposed by the first two or three reference moments are even more limiting than $\underline{\mathrm{DVH}}(t), \overline{\mathrm{DVH}}(t)$ above. In other words, the factual quality of approximating the reference DVH is superior to what is depicted in the figures. It is possible to derive the exact bounds on the DVH given the first two and three moments. However, these derivations are far more technical and do not serve the illustrative role we chose for the material in the appendix.

[8] Since the three-moment bounds are derived from the concentration inequalities—probability estimates on the deviation from the mean—in order to achieve monotone improvement in $\underline{\mathrm{DVH}}(t), \overline{\mathrm{DVH}}(t)$ as compared to the two-moment bounds, we superimpose these bounds with one other.

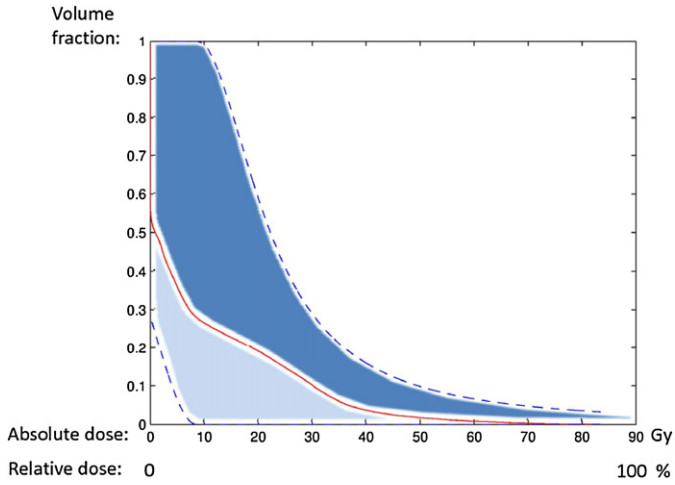

Figure A3. Area-based metrics 1 and 2: the mid solid curve is the reference DVH, two outer dashed curves are the moment-based bounds, upper darker shaded area corresponds to metric 2 and the sum of two shaded areas corresponds to metric 1.

Proximity metrics

In order to judge relative improvements or deficiencies of the moment-based error bounds $\underline{\mathrm{DVH}}(t), \overline{\mathrm{DVH}}(t)$, we introduce several proximity metrics—simply put, a set of numbers, computable from the reference DVH and its moments, that may be used to assess the quality of the moment-based approximation. These metrics, further combined with the visual representation of the DVH bounds, may serve as a valuable supplemental tool to a planner.

The quality of the moment-based approximation may be assessed via the *area*, and the *distance* between the bounding curves $\underline{\mathrm{DVH}}$, $\overline{\mathrm{DVH}}$. More precisely, we consider

(1) the area between $\underline{\mathrm{DVH}}$ and $\overline{\mathrm{DVH}}$,
(2) the largest area between the reference DVH and either $\underline{\mathrm{DVH}}$ or $\overline{\mathrm{DVH}}$,
(3) the distance between $\underline{\mathrm{DVH}}$ and $\overline{\mathrm{DVH}}$,
(4) the largest distance between the reference DVH and either $\underline{\mathrm{DVH}}$ or $\overline{\mathrm{DVH}}$,

see figures A3 and A4.

For simplicity of interpreting our metrics, we assume that the dose is measured in relative units— per cent of the maximal dose allowed in the plan—rather than in its absolute units such as Gy.

For a given reference DVH and the resulting moment-based bounds $\underline{\mathrm{DVH}}(t)$ and $\overline{\mathrm{DVH}}(t)$, where t is given in relative units and ranges from 0 to 1, metrics 1 and 2 may be easily computed by numerical integration. Note that due to the dose being presented in relative units, we know that the corresponding metrics' values range from 0 to 1, where the values close to 0 are clearly more preferred since 0 would imply the perfect reconstruction of the reference DVH.

Likewise, the values corresponding to metrics 3 and 4 may also be computed numerically relying on the two definitions, first of the distance from a point $z \in \Re^2$ to a compact set $S \subset \Re^2$,

$$\mathrm{dist}(z, S) = \min_{y \in S} \|z - y\|,$$

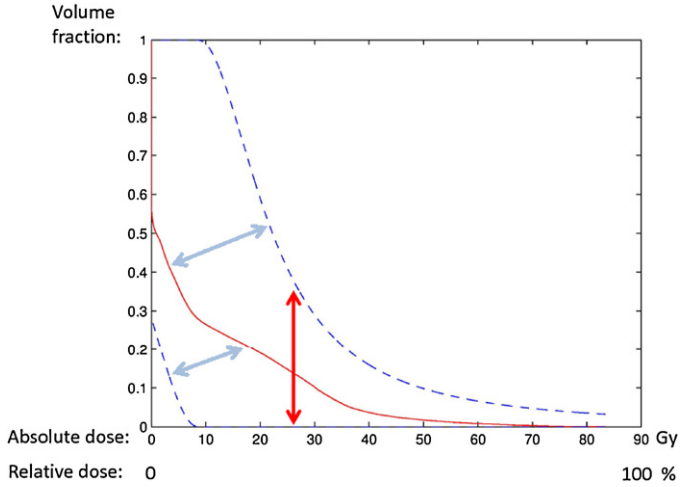

Figure A4. Distance-based metrics 3 and 4: the mid solid curve is the reference DVH, two outer dashed curves are the moment-based bounds, upper lighter arrow corresponds to metric 4 and the vertical arrow corresponds to metric 3.

Bounds / Metric	OAR, 2 moments	OAR, 3 moments	Target, 2 moments	Target, 3 moments
1	0.319729	0.261461	0.079687	0.078909
2	0.227941	0.182038	0.042750	0.042513
3	0.384536	0.319622	0.123170	0.116332
4	0.245285	0.228499	0.049764	0.049764

Figure A5. Metric values computed for two structures of interest.

and subsequently, the distance between two curves $\mathcal{C}_1, \mathcal{C}_2 \subset \Re^2$,

$$\text{dist}(\mathcal{C}_1, \mathcal{C}_2) = \max(\max_{z\in\mathcal{C}_1} \text{dist}(z, \mathcal{C}_2),\ \max_{z\in\mathcal{C}_2} \text{dist}(z, \mathcal{C}_1)),$$

where the reference DVH, $\underline{\text{DVH}}$ and $\overline{\text{DVH}}$ fulfil the roles of $\mathcal{C}_1$ and $\mathcal{C}_2$ curves, respectively. Note that again, due to dose scaling, these metrics' values range from 0 to $\sqrt{2}$, while the values close to 0 indicate a good quality of approximating the reference DVH. For illustration, we compute the values corresponding to metrics 1, 2, 3 and 4 for the exemplary reference DVHs considered with two and three-moment-based approximations and present these values in figure A5. As expected, the three-moment-based approximation outperforms the two-moment-based approximation.

References

Appenzoller L, Michalski J, Thorstad W, Mutic S and Moore K 2012 Predicting dose-volume histograms for organs-at-risk in IMRT planning *Med. Phys.* **39** 7446–61

Bednarz G, Michalski D, Houser C, Huq M, Xiao Y, Anne P and Galvin J 2002 The use of mixed-integer programming for inverse treatment planning with pre-defined field segments *Phys. Med. Biol.* **47** 2235–45

Bertsimas D and Popescu I 2005 Optimal inequalities in probability theory: a convex optimization approach *SIAM J. Optim.* **15** 780–804

Bortfeld T, Stein J and Preiser K 1997 Clinically relevant intensity modulation optimization using physical criteria *ICCR: Proc. 12th Int. Conf. on the Use of Computers in Radiation Therapy* vol 29 (Madison, WI: Med. Phys. Publishing) pp 1–4

Censor Y, Ben-Israel A, Xiao Y and Galvin J 2008 On linear infeasibility arising in intensity-modulated radiation therapy inverse planning *Linear Algebra Appl.* **428** 1406–20

Chen Y, Michalski D, Houser C and Galvin J 2002 A deterministic iterative least-squares algorithm for beam weight optimization in conformal radiotherapy *Phys. Med. Biol.* **47** 1647–58

Cho P S, Lee S, Marks R J M II, Oh S, Sutlief S G and Phillips M H 1998 Optimization of intensity modulated beams with volume constraints using two methods: Cost function minimization and projections onto convex sets *Med. Phys.* **25** 435–43

Dai J and Zhu Y 2003 Conversion of dose-volume constraints to dose limits *Phys. Med. Biol.* **48** 3927–41

Deasy J 1997 Multiple local minima in radiotherapy optimization problems with dose–volume constraints *Med. Phys.* **24** 1157–61

Langer M, Brown R, Urie M, Leong J, Stracher M and Shapiro J 1990 Large scale optimization of beam weights under dose-volume restrictions *Int. J. Radiat. Oncol. Biol. Phys.* **18** 887–93

Langer M and Leong J 1987 Optimization of beam weights under dose-volume restrictions *Int. J. Radiat. Oncol. Biol. Phys.* **13** 1255–60

Li N, Zarepisheh M, Tian Z, Uribe-Sanchez A, Zhen X, Graves Y, Gautier Q, Zhou L, Jia X and Jiang S 2012 IMRT Re-planning by adjusting voxel-based weighting factors for adaptive radiotherapy *Med. Phys.* **39** 3966

Michalski D, Xiao Y, Censor Y and Galvin J M 2004 The dose–volume constraint satisfaction problem for inverse treatment planning with field segments *Phys. Med. Biol.* **49** 601–16

Morrill S M, Lane R G, Wong J A and Rosen I I 1991 Dose-volume considerations with linear programming optimization *Med. Phys.* **18** 1201–10

Romeijn H, Ahuja R, Dempsey J and Kumar A 2006 Optimal multileaf collimator leaf sequencing in IMRT treatment planning *Oper. Res.* **54** 201–16

Spirou S and Chui C 1998 A gradient inverse planning algorithm with dose-volume constraints *Med. Phys.* **25** 321–33

Starkschall G, Pollack A and Stevens C 2001 Treatment planning using a dose–volume feasibility search algorithm *Int. J. Radiat. Oncol. Biol. Phys.* **49** 1419–27

Wu B, Ricchetti F, Sanguineti G, Kazhdan M, Simari P, Jacques R, Taylor R and McNutt T 2011 Data-driven approach to generating achievable dose–volume histogram objectives in intensity-modulated radiotherapy planning *Int. J. Radiat. Oncol. Biol. Phys.* **79** 1241–7

Wu Q and Mohan R 2000 Algorithms and functionality of an intensity modulated radiotherapy optimization system *Med. Phys.* **27** 701–11

Yan D, Vicini F, Wong J and Martinez A 1999 Adaptive radiation therapy *Phys. Med. Biol.* **42** 123–32

Zarepisheh M and Khorram E 2011 On the transformation of lexicographic nonlinear multiobjective programs to single objective programs *Math. Methods Oper. Res.* **74** 217–31

Zarepisheh M, Uribe-Sanchez A, Li N, Jia X and Jiang S 2012 A multi-criteria framework with voxel-dependent parameters for radiotherapy treatment plan optimization *Med. Phys.* **39** 3919

Zhang Y and Merritt M 2008 Dose-volume-based IMRT fluence optimization: a fast least-squares approach with differentiability *Linear Algebra Appl.* **428** 1365–87

Zinchenko Y, Craig T, Keller H, Terlaky T and Sharpe M 2008 Controlling the dose distribution with gEUD-type constraints within the convex radiotherapy optimization framework *Phys. Med. Biol.* **53** 3231–50